

Generation of α -linolenic acid microparticles from silkworm pupae oil by microfluidic droplet

Zhi-Yuan Bai¹, Shu-Meng Zhang¹, Xi Liu¹, Sheng Sheng^{1,2,3,4}, Jun Wang^{1,2,3,4,*}, Fu-An Wu^{1,2,3,4,*}

¹ School of Biotechnology, Jiangsu University of Science and Technology, Zhenjiang 212018, PR China;

² Sericultural Research Institute, Chinese Academy of Agricultural Sciences, Zhenjiang 212018, PR China;

³ Key Laboratory of Silkworm and Mulberry Genetic Improvement, Ministry of Agriculture, Sericultural Research Institute, Zhenjiang 212018, PR China;

⁴ Jiangsu Key Laboratory of Sericultural Biology and Biotechnology, Zhenjiang 212018, PR China.

* Corresponding author. *E-mail*: wangjun@just.edu.cn; fuword@163.com (Prof. Dr. J. Wang, Prof. Dr. Fuan Wu).

ABSTRACT: Caffeic acid grafted chitosan (CA-g-Ch) was successfully synthesized as a novel wall material and used to embed α -linolenic acid (ALA) by microfluidic droplet technology. The shear force and viscosity of CA-g-Ch were determined, the effects of Tween 20 concentrations on the morphology and size of droplet formatted were investigated, and the microcapsules were characterized by IR, XRD and SEM. The results indicated that CA-g-Ch has lower viscosity and stronger emulsification properties than chitosan, and its solution has good fluidity. The diameter of the droplets prepared with 0.25% concentration of Tween 20 was 18.96 μm , and had obvious monodispersity. The droplets cannot form normally when the concentration is higher than 1%. The ALA microcapsules were successfully prepared using freeze-dried droplets. When the Tween 20 concentration was 0.25%, the antioxidant activity of ALA microcapsules (ALA-M) by DPPH method was 7.2 times higher than that of the ALA untreated.

KEYWORDS: α -linolenic acid; co-valent grafting; oxidative stability; antioxidant; microfluidic; microparticle.

Introduction

Many reports have shown that α -linolenic acid (ALA) and long-chain metabolites play a crucial role in many physiological metabolic activities [1]. So, some food science laboratories and food processors have come forward with novel functional food products, fortified with ALA. However, ALA has shortcomings such as easy oxidation, deterioration and inconvenience of application. Usually, oxygen absorbents used to remove oxygen in contact with oil, nitrogen filled protection and adding antioxidants to the oil were three common methods of protecting the oil from oxidation [2]. The first two methods are effective in preventing linolenic acid from being oxidized during storage. The protective of the oxygen absorbing agent and nitrogen was weakened while the sealed containers was open, resulting in direct contact between linolenic acid and air. Moreover, antioxidants can have relatively better antioxidant effects, but there are also drawbacks such as side effects of toxicity and poor thermal stability. Therefore, a new technique for fortification of ALA in food products was desired.

Microfluidic technology was widely employed to deal with chemical and biological fluids accurately at the microscale. The microfluidic technology can be used in the shape of medical package, drug synthesis and pharmaceutical distribution in the decades [3]. Thus, microfluidic has been considered as a promising technique for such fortification of ALA in food products, as it imparts controlled release behavior and protect against oxidation during processing, handling and storage [4]. Currently, droplet microfluidic is an important branch of microfluidics. It can generate and manipulate highly monodisperse droplets, emulsions, double emulsions, and bubbles [5]. With this technology, it is ideal for performing chemical and biochemical reactions in a high flux and automatic way in droplets.

Emulsifier and wall material are important factors that ensure the success of the microencapsulation process [6]. Chitosan, a versatile amino polysaccharide with excellent film forming and emulsifying properties has been employed frequently as a wall material, as well as an emulsifier for microencapsulation of unsaturated oils [7]. As a poly cationic polysaccharide, chitosan has been observed to surround oil-in-water (o/w) emulsion droplets and repel pro-oxidant metals in the surrounding environment. So far, chitosan employed as a bio-functional natural polysaccharide has been reported [8], dietary supplementation of chitosan may result in health promoting effects such as hypolipidemic and cardio-protective activities [9]. Therefore, grafting of chitosan with various functional moieties was investigated for improving the bioactivity, modulate solubility and emulsifying properties of chitosan.

In the present study, the application of CA-g-Ch for microencapsulation of ALA was firstly investigated. The antioxidant properties of CA-g-Ch can enhance the oxidative stability of the encapsulated ALA and the microparticles could be a new functional food ingredient. Thus, the aim of this study is to utilize CA-g-Ch as a new antioxidant wall material and prepare oil-in-water emulsion droplets of ALA by microfluidic technology.

Materials and Methods

Synthesis and characterization of CA-g-Ch

CA-g-Ch was synthesized according to the reference [10]. In a 1 L three-neck round-bottomed flask, 5g of chitosan was dissolved in 1 L of 2% acetic acid solution (v/v). 10 mL of 1 M H₂O₂ containing 0.54 g of ascorbic acid was added to the chitosan solution. CA (0.1 w/v) was dissolved in the ethanol and then added to the mixed solution. With constant stirring, the reaction was maintained at 25 °C in a nitrogen atmosphere for 24 h. To remove unreacted phenolic acids, the mixture was dialyzed in distilled water for 72 h. To confirm that the free CA was completely removed, the reaction mixture and pure CA were compared in a silica-coated TLC plate. Finally, the dialysate was freeze dried to yield CA-g-Ch derivative in solid form. FTIR spectra were recorded on a 670-IR+610-IR Fourier Transformation Infrared Spectrophotometer (Varian, Salt Lake City, USA). The derivative was solubilized in D₂O before recording ¹H nuclear magnetic resonance (Bruker BioSpin, Switzerland). CA-g-Ch was determined by an XL-30 Environmental Scanning Electron Microscope (Philips, Amsterdam, Holland). The grafting ratio of CA on chitosan was estimated using liquid chromatography method [11].

Rheology of CA-g-Ch

Rheological measurements of chitosan and CA-g-Ch were performed on a AR-G2 Rotational Rheometer (TA Instruments, New Castle, USA) with a cone and plate geometry (cone diameter = 50 mm, angle = 4°, gap = 0.05 mm) while the temperature was adjusted at 25 °C. Experimental flow curves were fitted to a power law model as shown in Eq 1.

$$\eta = K\dot{\gamma}^{n-1} \quad (1)$$

where η was the viscosity (Pa·s), $\dot{\gamma}$ was the shear rate (s⁻¹), K was the consistency index (Pa·sⁿ) and n was the index that provided information about the flow behavior related to the effect of shear rate.

Preparation of o/w emulsion

CA-g-Ch (0.8 % wt/v) was dissolved in acetate buffer solution (2 mM sodium acetate and 98 mM acetic acid in water, pH 3.0) with overnight stirring on a magnetic stirrer. To prepare the o/w emulsion droplets of ALA (isolated from silkworm pupa oil by the Simulated Moving Bed Chromatography), using a Constant Pressure Microfluidic Pump System. Pump 1 (0.75 μ L/min) in the microfluidic pressure pump system is continuously fed into the continuous phase (CA-g-Ch solution) and pump 2 (0.45 μ L/min) is continuously fed into the disperse phase (mixing ALA and 0.25% wt/v Tween 20 solution) to prepare an o/w emulsion of ALA. The resulting droplets were observed under a microscope for their morphological characteristics, and the flow rates of the continuous phase and the dispersed phase were controlled by pump [12].

Characterisation of the o/w emulsion

The microstructure of the matured emulsions was observed on an optical microscope at an objective magnification of 40X. The images were captured by software for the digital image processing. The Size distribution by number of the emulsion droplets, poly dispersity index (PDI) were measured on a Malvern Mastersizer 2000 Particle Analyzer (Malvern Instruments Ltd., Malvern, England). The emulsions were not diluted before analysis. A polydisperse model was used to analyse the data presented as size distribution by number. Particle size was expressed as Z average hydrodynamic diameter (d. nm)

Freeze-drying of o/w emulsion

The optimized emulsion was up-scaled and freeze-dried using a freeze dryer to obtain the microparticles loading with ALA. The freeze dryer temperature was -40 °C. The obtained powder was immediately transferred into a glass jar for further characterization study.

Characterization of ALA-M

Samples were mounted on metal stubs with the help of double backed adhesive tapes, examining them under an SEM. X-Ray powder diffraction data of the samples were recorded on an X-Ray Diffraction Instrument (Bruker AXS, Karlsruhe, Germany) over a 2 θ range from 3 to 40°, using a scan rate of 0.04° min⁻¹. In order to study the thermal behavior of ALA-M. Thermogravimetric analysis (STA-449F4N TGA, Netzsch, Freistaat Bayern, Germany) was used to measure the degradation and decomposition of ALA-M [13]. The measurements were carried out in the temperature of 30-800 °C, at a heating rate of 10 °C min⁻¹ and the nitrogen gas flow was 20 mL min⁻¹.

Determination of encapsulation efficiency

The ALA (50 mg) dissolving in absolute alcohol fixed volume to 100mL, and the 0.5mg / mL stock solution was prepared. Accurately measure 0.2, 0.4, 0.6, 0.8, 1 mL reserve liquid to 10 mL brown capacity bottle, and use ethanol to determine volume as liquid. Using absolute ethanol as blank control, the absorbance was measured at the

325nm wavelength, and the standard curve equation of absorbance and mass concentration was Eq 2.

$$Y = 8.4193X - 0.0401 \quad (R^2 = 0.99) \quad (2)$$

According to the method described by Keawchaon et al [14], the content of ALA was determined by ultraviolet spectrophotometry. Take 100 mL ALA-M suspension in 10 mL centrifuge tube, add 5 mL 2 mol/L HCl solution, boil 30min at 95 centigrade, cool, add 1 mL anhydrous ethanol, and use high speed centrifuge at 25 °C, 9000 rpm under centrifugal 5min. The supernatant was measured with a UV spectrophotometer in the range of 200-400 nm wavelengths, and the content of ALA could be obtained by the absorption of the ALA solution standard curve and the absorbance of the 325 nm wavelength. The same volume of blank chitosan suspension was used as blank sample in the same way. The entrapment efficiency (encapsulation efficiency, EE) was calculated by Eq 3, M1 is the total mass/mg of ALA in the system; M2 is the free ALA mass/Mg in the system [6].

$$EE (\%) = \frac{(M1 - M2)}{M1} \times 100 \quad (3)$$

In vitro release behavior

In vitro release behavior of ALA-M was investigated using a simulated gastrointestinal model according to the method given by Burgar et al [15], with slight modifications. Simulated gastric fluid (SGF) was prepared by dissolving 2.0 g of NaCl and 7.0 ml of 36% HCl in 900 ml of water. After the addition of 5.0 g of pepsin, the solution pH was adjusted to 1.2 with 0.1 M HCl and the final volume was made up to 1 L with water. Simulated intestinal fluid (SIF) was prepared by dissolving 6.8 g of K₂HPO₄ in 800 ml of water. To this solution, 77 ml of 0.2 M NaOH and 100.0 g of pancreatin was added followed by stirring overnight at 4 °C. Solution pH was adjusted to 6.8 with 1 M NaOH or 1 M HCl and the final volume was made up to 1 L with water.

Determination of antioxidant activity

ALA o/w droplets were collected, and the ALA antioxidant properties were investigated by the DPPH method, as described by Burits and Bucar with slight modification [16]. The specific measure is to dilute ALA o/w droplets and ALA to prepare a sample solution. 2 mL DPPH solution and 2 mL sample solution were added to the test tube, shaken, and allowed to stand for 30 min in the dark, centrifuged at 3000 rpm for 10 min, zeroed with absolute ethanol, and measured the absorbance (A_i) of the supernatant at 517 nm. At the same time, the absorbance (A_c) of 2 mL of DPPH solution and 2 mL of absolute ethanol was measured. And 2 mL of the sample solution was mixed with 2 mL of absolute ethanol. The reaction was carried out for 30 min, followed by centrifugation at 3000 rpm for 10 min. The absorbance (A_j) of the supernatant was measured. The scavenging power is expressed in terms of EC₅₀ (%). The EC₅₀ (%) was calculated using the Eq 4.

$$EC_{50} \% = \left[1 - \frac{A_i - A_c}{A_j} \right] \times 100 \quad (4)$$

Results and Discussion

Synthesis and characterization of CA-g-Ch

Among the different synthesis methods reported for chitosan grafting of phenolic acids, free radical-mediated grafting of phenolic acids is considered to be the fastest, economical, and eco-friendly [17]. The yield of CA-g-Ch varied between 55 and 70 %. No spot corresponding to CA was observed on the developed TLC plates for CA-g-Ch, confirming the absence of free CA and successfully grafting on chitosan. FTIR spectra of chitosan exhibited major characters banded at around 3428 cm⁻¹ (OH), 2883 cm⁻¹ (C-H stretching), 1650 cm⁻¹ (amide I), 1550 cm⁻¹ (amide II), 1072 cm⁻¹ (COC) and 899 cm⁻¹ (pyranose ring) (see Fig. 1).

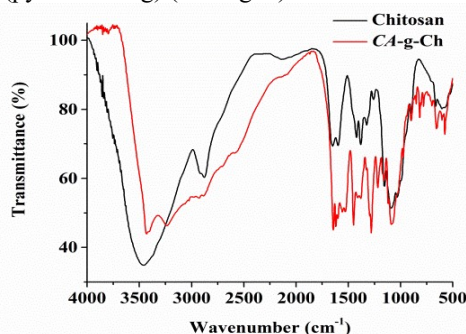


Fig. 1. FTIR spectra and structure assignment of chitosan and CA-g-Ch

Compared to chitosan, intensity of amide I (at around 1644 cm^{-1}) and amide II (at around 1549 cm^{-1}) bands in CA-g-Ch were both increased, which means that new amide linkage was produced. It confirms successful grafting of CA onto chitosan. The grafting ratio of CA on chitosan was $379\text{ mg CA equivalent/g}$ of polymer using liquid chromatography,

Effect of two-phase flow rate on droplet size

Fig. 2a shows the influence of continuous phase flow rate in a microfluidic droplet reactor on its ALA emulsion droplets. When the flow rate of the dispersed phase was constant, the continuous increase in the flow rate of the continuous phase will reduce the aspect ratio of the generated droplet. When the flow rate of the dispersed phase was $0.5\text{ }\mu\text{L}/\text{min}$, the droplet aspect ratio decreased from 2.8 ± 0.6 to 0.8 ± 0.2 with the increase of the continuous phase flow rate. This is because the width of the channel in the microchip was fixed, and when the flow rate increases, the continuous phase squeezes the dispersed phase so that the droplet length was reduced, so that the prepared droplet was correspondingly smaller (drop diameter from $37.3\pm 2.73\text{ }\mu\text{m}$ to $25.6\pm 5.21\text{ }\mu\text{m}$). As the discrete phase flow rate increased, the shear rate of the continuous phase and the inertial force of the fluid increased [12]. So that the droplet generation speed is increased, and the high-speed flow of the two phases increases the droplet generation speed, reduces the period of droplet generation, and the droplet size also becomes smaller.

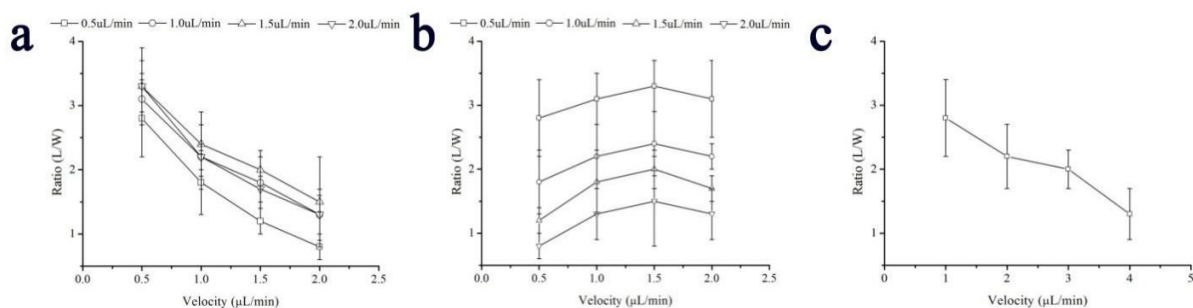


Fig. 2. The relationship between the formation of droplets and the two different phases. (a) The relationship between continuous phase velocity and droplets size; (b) The relationship between dispersed phase velocity and droplets size; (c) The relationship between total velocity and droplets size.

Fig. 2b shows the effect of dispersed phase flow rate in a microfluidic droplet chip on the preparation of ALA emulsion droplets. It can be seen that when the flow rate of the continuous phase is constant, the flow rate of the dispersed phase is continuously increased, and the aspect ratio of the droplet gradually increases. When the continuous phase flow rate was $0.5\text{ }\mu\text{L}/\text{min}$, the droplet length-width ratio increased from 2.8 ± 0.6 to 3.3 ± 0.4 with the increase of the dispersion flow rate, but the droplets could not be formed and be dispersed with the further increase of the dispersion flow rate. The fluid flows out of the chip. This phenomenon appears due to the fact that when the flow rate of the discrete phase increases, the resistance to the continuous phase also increases, and the continuous phase takes longer to pinch off the dispersed phase to form droplets, so the resulting droplet size will be large. When the continuous phase cannot pinch off the dispersed phase, droplets cannot form [18].

When both the continuous phase and dispersed phase flow rates are the same, the sum of the continuous phase flow rate and the dispersed phase flow rate was changed. Fig. 2c shows the effect of total velocity in a microfluidic droplet chip on the preparation of ALA emulsion droplets. It can be seen that when the ratio of the dispersed phase to the continuous phase was constant, changing the overall flow rate, the resulting droplet size changed with the change of the total flow rate. As the overall flow rate increases, the droplets were always reduced in aspect ratio due to the extrusion of the external fluid. However, the droplet size decreased first and then became larger. At a total flow rate of $1\text{ }\mu\text{L}/\text{min}$, the droplets generated were the largest with a diameter of $37.3\pm 2.73\text{ }\mu\text{m}$. At a total flow of $3\text{ }\mu\text{L}/\text{min}$, the resulting droplets were the smallest with a diameter of $32.1\pm 2.96\text{ }\mu\text{m}$. When the overall flow rate was further increased, the droplet diameter increased. This may be because when the continuous phase and the discrete phase had large flow rates, the droplets were formed too quickly, and a plurality of small droplets partially polymerize in the generated microchannel, so that the overall size of the droplets became large.

Optimisation of o/w emulsion

The combination of chitosan with anionic and non-ionic emulsifiers can stabilize the o/w emulsion better than using it alone [19]. Especially Tween 20, a non-ionic emulsifier was found suitable for binding with chitosan to stabilize the o/w emulsion. The oil droplets stabilized by Tween 20 are negatively charged and therefore

electrostatically interact with cationic chitosan molecules to form a second protective wall material [20]. Consequently, Tween 20 was used in the combination with CA-g-Ch for stabilisation of the o/w emulsion. The effect of chitosan concentration on its emulsifying ability was studied. It was found that the emulsifying activity of chitosan is highest at the concentration of 0.75% and thereafter decreases with increasing concentration [21].

Considering this, the o/w emulsion was prepared by a concentration of 0.8% of CA-g-Ch. Fig. 3 shows micrograph of emulsion containing Tween 20. Various concentrations of Tween 20 (1.0, 0.5, 0.25, and 0.1% w/v) were evaluated prior to freeze-drying to achieve best emulsion stability. The droplets at a concentration of 0.25% Tween 20 were uniform in size (29 μm) and there was no emulsion polymerization occurred. However, with the concentration of Tween 20 increased, the droplets began to polymerize, indicating that the emulsification effect began to decrease. The emulsification activity of chitosan was highest when the concentration of Tween 20 was 0.25%, and then decreased as the concentration increased. Thus, 0.25% Tween 20 was used to prepare the o/w emulsion. However, these droplets started to break down after a long period of time and delamination occurred again. Therefore, the emulsion cannot be a delivery vehicle for ALA. This further proves the need to freeze-dry the emulsion to give it physical and oxidative stability.

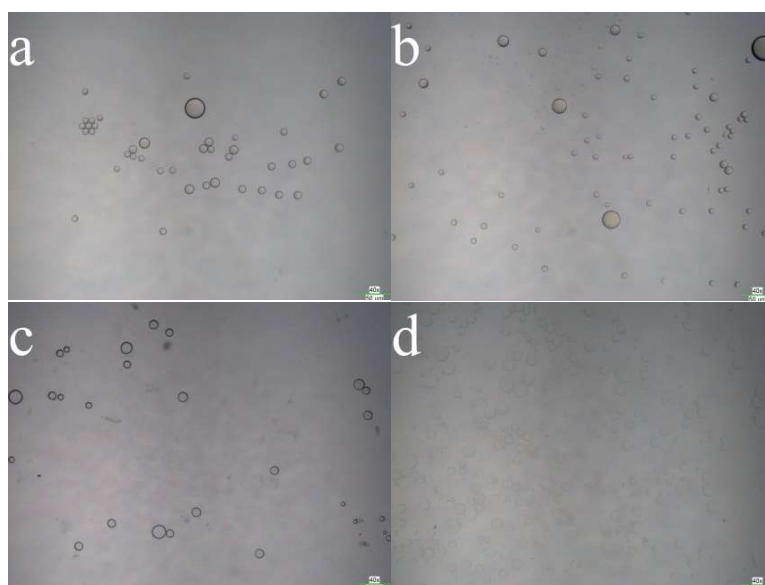


Fig. 3. Micrograph of emulsion containing Tween 20. (a) 0.1% Tween 20; (b) 0.25% Tween 20; (c) 0.5% Tween 20; (d) 1.0% Tween 20.

Particle size distribution, morphology and crystallinity of ALA-M

Fig. 4 shows SEM images of CA-g-Ch and ALA-M. For CA-g-Ch (Fig. 4a), the solid was filmy and the surface is smooth and wrinkle-free; For ALA-M (Fig. 4b), there were some granular objects and holes in the surface, which indicates that the ALA oil was encapsulated inside the wall material.

Fig. 4. SEM images of the ALA-M. (a) CA-g-ch at X1000; (b) ALA-M at X2000.

In addition, the crystallization behavior of CA-g-Ch and ALA-M was investigated by XRD. As shown in Fig. 5, the intensity of the reflection of CA-g-Ch at 2θ 20° is significantly reduced and the peak shifts to shorter angles due to the introduction of CA in the chitosan structure. Further, CA-g-Ch exhibited new low intensity peaks at 2θ 13° ,

18°, 26° and 29° due to the formation of new covalent bonds and changes in chitosan structure, the crystallinity decreased. It is consistent with previous reports. The change in chitosan may be due to the large amount of CA that destroys its internal hydrogen bonds [22]. ALA-M show a further decrease in peak intensity at 2θ 20°, while low intensity peaks at 2θ 13°, 18° disappeared, and new intensity peaks appeared at 35° and 40°. This may be due to further folding of the polymer chains and successful encapsulation of the ALA within the CA-g-Ch microparticles.

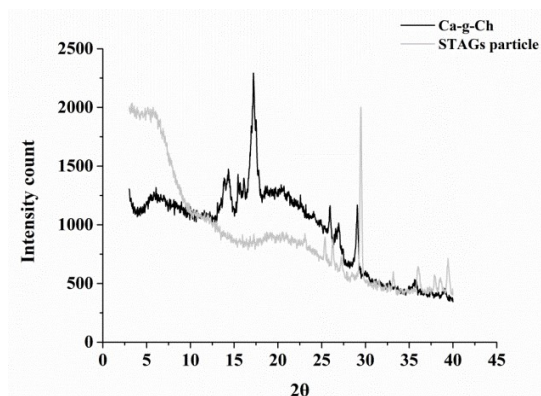


Fig. 5. X-ray diffractograms of chitosan, CA-g-Ch and ALA encapsulate.

The TGA of ALA-M

The thermogravimetric (TG) curves were used to determine the thermal degradation and thermal stability of ALA-M (Fig. 6). The thermal decomposition of each sample took place in a programmed temperature range of 25 °C to 800 °C. The ALA-M showed six stages of weight loss process [13]. As illustrated in Table 1, the degradation steps were in the temperature range of 26.59-102.80 °C, 102.80-166.23 °C, 166.23-255.27 °C, 255.27-367.68 °C, 367.68-504.57 °C and 505.68-793.22 °C. The percentage of the loss weight composites at corresponding transition was 5.3 %, 5.5 %, 24.8 %, 24.9 %, 15.1 % and 7.8%, respectively. Therefore, more stages suggested that a higher value of the thermal stability it will have.

Fig. 6. The TG analysis of ALA-M

Table 1 Results of the TG analysis ALA.

Sample	No. of transition	Transition temperature (°C)			Weight loss at transition (%)	Residual weight (%) at 800 °C
		T _i	T _m	T _f		
ALA-M	1	26.59	54.81	102.80	5.30	83.82
	2	102.80	147.68	166.23	5.51	
	3	166.13	224.33	255.27	24.82	
	4	255.27	291.57	367.68	24.90	
	5	367.68	401.89	504.57	15.10	
	6	504.68	604.01	793.22	7.83	

Encapsulation efficiency of the process

EE value between 60-90% are generally considered satisfactory in published literature depending on the type and composition of wall material, drying processes used and the stability of the feed emulsion [23]. The EE value recorded in this study was 79%, it's fully meet the needs of use [24]. This could be due to better emulsifying property of CA-g-Ch. And droplet microfluidic technology provides higher stability, making ALA encapsulated process on an even keel. The satisfactory EE values obtained in this study prove successful encapsulation of ALA in CA-g-Ch microparticles and suitability of further application in food.

In vitro release behaviour

Percentage release of ALA from ALA-M exposure to SGF and SIF was presented. Percentage of ALA released increased slowly as time of exposure increased from 2 to 6 h. Higher percentage release of ALA in case of sequential exposure to SGF and SIF than in SGF exposure alone was obvious and consistent with earlier observations [25]. It was noticed that maximum 56% release of ALA was recorded under exposure to SGF and SIF for 6 h. It showed that ALA was continuously released from ALA-M.

Antioxidant activity

In order to investigate the antioxidant capacity of ALA o/w droplets, the antioxidant properties were measured by DPPH method. As shown in Table 2, the EC₅₀ values of the ALA droplets and samples were 84.96±4.05% 12.03±4.17%, respectively. The EC₅₀ value of ALA droplet was 7.06 times than that of the non-droplet form. The EC₅₀ value can indicate the antioxidant activity of a substance, the larger the value, the more difficult it is for ALA to oxidize [26]. Therefore, the ALA o/w droplets can reduce the oxidative deterioration of ALA. This is because the outer layer of water cuts off the direct contact between oxygen and its internal ALA and acts to slow the oxidation of ALA.

Table 2 The EC₅₀ values of DPPH experiments of ethyl ALA and its droplet.

Sample	EC ₅₀ (%)
ALA o/w droplets	84.96±4.05 ^a
ALA	12.03±4.17 ^b

Data with different small letters in the same list are significantly different at 0.05 level.

Conclusions

The microfluidic droplet technique with anti-oxidation wall material was constructed to prepare monodisperse ALA-M. CA-grafted chitosan was prepared from CA and chitosan. The aqueous solution of CA-g-Ch was used as the aqueous phase to prepare monodispersed droplets of ALA by microfluidic droplet technology. The 0.25% Tween 20 solution was used to prepare O/W droplets with an encapsulation efficiency of 79%. This capsule obtained after drying was uniform size, stable morphology, good rheological properties and high dispersion. In addition, ALA-M showed excellent antioxidant properties (EC₅₀ = 86.94±4.05 %).

Acknowledgments

This study was financially supported by the Natural Science Research General Project of Jiangsu Province Universities (2017120206), the Key Research and Development Program (Modern Agriculture) of Jiangsu Province (BE2017322), the Six Talent Peaks Project of Jiangsu Province (2015-NY-018), the Qing Lan Project of Jiangsu Province (2014), and the Shen Lan Young scholars program of Jiangsu University of Science and Technology (2015).

References

1. Roger M. Loria, David A. Padgett.: α -Linolenic acid prevents the hypercholesteremic effects of cholesterol addition to a corn oil diet. *Journal of Nutritional Biochemistry*, **8**(3), 140-146 (1997)
2. H. Akhtar, I. Tariq, S. Mahmood et al. Effect of antioxidants on stability, nutritional values of refined sunflower oil during accelerated storage and thermal oxidation in frying. *Bangladesh Journal of Scientific & Industrial Research*, **47**(47), 223-230 (2012)
3. A. D. Griffiths, D. S. Tawfik.: Miniaturising the laboratory in emulsion droplets. *Trends in Biotechnology*, **24**(9), 395-402 (2006)
4. T. Ghorbanzade, S. M. Jafari, S. Akhavan et al.: Nano-encapsulation of fish oil in nano-liposomes and its application in fortification of yogurt. *Food Chemistry*, **216**, 146-152 (2017)
5. Michinao Hashimoto, Sergey S. Shevkopyas, Beata Zasońska et al.: Formation of Bubbles and Droplets in Parallel, Coupled Flow-Focusing Geometries. *Small*, **4**(10), 1795-1805 (2008)
6. Laura G. Hermida, Gabriela Gallardo.: Food Applications of Microencapsulated Omega-3 Oils, (2015)

7. Zhiping Shen, Mary Ann Augustin, Luz Sanguansriet al.: Oxidative Stability of Microencapsulated Fish Oil Powders Stabilized by Blends of Chitosan, Modified Starch, and Glucose. *Journal of Agricultural & Food Chemistry*, **58**(7), 4487 (2010)
8. Rangasamy Anandan, Niladri Sekhar Chatterjee, Ramalingam Sivakumaret al.: Dietary Chitosan Supplementation Ameliorates Isoproterenol-Induced Aberrations in Membrane-Bound ATPases and Mineral Status of Rat Myocardium. *Biological Trace Element Research*, **167**(1), 103-109 (2015)
9. Wei Zhang, Jiali Zhang, Qixing Jianget al.: The hypolipidemic activity of chitosan nanopowder prepared by ultrafine milling. *Carbohydrate Polymers*, **95**(1), 487-491 (2013)
10. Niladri Sekhar Chatterjee, Rangasamy Anandan, Mary Navithaet al.: Development of thiamine and pyridoxine loaded ferulic acid-grafted chitosan microspheres for dietary supplementation. *Journal of Food Science & Technology*, **53**(1), 551-560 (2016)
11. Sha-Sha Wang, Zhong-Jian Li, Sheng Shenget al.: Microfluidic biocatalysis enhances the esterification of caffeic acid and methanol under continuous - flow conditions. *Journal of Chemical Technology & Biotechnology*, **91**(2), 555-562 (2016)
12. Micheal Armani, Satej Chaudhary, Roland Probstet al.: Control of microfluidic systems: two examples, results, and challenges. *International Journal of Robust & Nonlinear Control*, **15**(16), 785-803 (2005)
13. J. P. Siregar, M. S. Salit, M. Z. Ab Rahmanet al.: Thermogravimetric analysis (TGA) and differential scanning calorimetric (DSC) analysis of pineapple leaf fibre (PALF) reinforced high impact polystyrene (HIPS) composites. *Pertanika Journal of Science & Technology*, (2011)
14. L. Keawchaoon, R. Yoksan. Preparation.: characterization and in vitro release study of carvacrol-loaded chitosan nanoparticles. *Colloids & Surfaces B Biointerfaces*, **84**(1), 163-171 (2011)
15. M. Iko Bugar, Pamela Hoobin, Rangika Weerakkodyet al.: NMR of Microencapsulated Fish Oil Samples During In Vitro Digestion. *Food Biophysics*, **4**(1), 32-41 (2009)
16. P. Calvo, C. Remuñán López, J. L. Vila Jatotet al. Novel hydrophilic chitosan - polyethylene oxide nanoparticles as protein carriers. *Journal of Applied Polymer Science*, **63**(1), 125-132 (1997)
17. W. Pasanphan, G. R. Buettner, S. Chirachanchai.: Chitosan gallate as a novel potential polysaccharide antioxidant: an EPR study. *Carbohydrate Research*, **345**(1), 132-140 (2010)
18. T. Nisisako, T. Torii, T. Higuchi.: Droplet formation in a microchannel network. *Lab on A Chip*, **2**(1), 4 (2002)
19. Yue Li, Lianzhong Ai, Wallace Yokoyamaet al.: Properties of Chitosan-Microencapsulated Orange Oil Prepared by Spray-Drying and Its Stability to Detergents. *Journal of Agricultural & Food Chemistry*, **61**(13), 3311-3319 (2013)
20. S. Mun, E. A. Decker, D. J. McClements.: Influence of droplet characteristics on the formation of oil-in-water emulsions stabilized by surfactant-chitosan layers. *Langmuir*, **21**(14), 6228-6234 (2005)
21. X. Li, W. Xia.: Effects of concentration, degree of deacetylation and molecular weight on emulsifying properties of chitosan. *International Journal of Biological Macromolecules*, **48**(5), 768-772 (2011)
22. S. Woranuch, R. Yoksan.: Preparation, characterization and antioxidant property of water-soluble ferulic acid grafted chitosan. *Carbohydrate Polymers*, **96**(2), 495-502 (2013)
23. N. Hardas, S. Danviriyakul, J. L. Foleyet al.: Accelerated stability studies of microencapsulated anhydrous milk fat. *LWT - Food Science and Technology*, **33**(7), 506-513 (2000)
24. R. G. Kumar L, N. S. Chatterjee, C. S. Tejpalet al.: Evaluation of chitosan as a wall material for microencapsulation of squalene by spray drying: Characterization and oxidative stability studies. *International Journal of Biological Macromolecules*, (2017)
25. Ankit Goyal, Vivek Sharma, Manvesh Kumar Sihaget al.: Effect of microencapsulation and spray drying on oxidative stability of flaxseed oil and its release behavior under simulated gastrointestinal conditions. *Drying Technology*, **7**, (2015)
26. JA Larrauri, A. Concepción Sánchezmoreno, F. Sauracalixto. Effect of temperature on the free radical scavenging capacity of extracts from red and white grape pomace peels. *Journal of Agricultural & Food Chemistry*, **46**(7), 2694-2697 (1998)